Random Walking during Quiet Standing

J. J. Collins* and C. J. De Luca

NeuroMuscular Research Center and Department of Biomedical Engineering, Boston University, 44 Cummington Street, Boston, Massachusetts 02215

(Received 30 March 1994)

During quiet standing, the human body continually moves about in an erratic, and possibly chaotic, fashion. Here we show that postural sway is indistinguishable from correlated noise and that it can be modeled as a system of bounded, correlated random walks. These novel results suggest that the postural control system incorporates both open-loop and closed-loop control mechanisms.

PACS numbers: 87.45.Dr, 05.45.+b

Noiselike fluctuations abound in physiological systems and processes [1]. It has been suggested that the complex, unpredictable behavior exhibited by the mammalian nervous [2] and muscular systems [3] may be instances of deterministic chaos. A likely candidate for physiological chaos is the human postural control system, the output of which is highly irregular [4], as illustrated in Fig. 1. The identification of postural sway as an instance of chaos would suggest that there is a simple, dynamical mechanism at work in balance regulation and may make possible new therapeutic and preventative strategies for postural instability.

Chaotic systems are typically characterized by the existence of an attractor that has a fractal structure and a sensitive dependence upon initial conditions. Numerical algorithms which quantify either of these properties have been developed to detect the presence of deterministic chaos in experimental time series [5–7]. (In the case of scalar time series, such algorithms usually require one to reconstruct first the system's attractor by embedding the time series in m-dimensional phase space [8].) The most common way to approximate the fractal structure of a system's attractor is to calculate the correlation dimension, D_2 [5]. Chaotic systems are generally characterized by finite, noninteger, i.e., fractal, values for D_2. To compute D_2, one first calculates the correlation sum, $C(\varepsilon)$, which is the fraction of pairs of points (on the reconstructed attractor) that are separated by a distance less than ε, for various values of ε. The correlation dimension can then be determined from the slope of a suitable, linear scaling region in the plot of $\ln C(\varepsilon)$ versus $\ln\varepsilon$. A system's sensitivity to initial conditions can be quantified by computing its Lyapunov characteristic exponents. Lyapunov exponents provide a measure of the rate at which initially nearby trajectories on an attractor diverge or converge as time progresses. The presence of a positive Lyapunov exponent is sufficient for diagnosing chaos and reflects the fact that nearby trajectories diverge at an exponential rate. For experimental time series, the largest Lyapunov exponent λ_1 can be determined from the slope of a suitable, linear scaling region in the plot of $\langle \ln d_j(i) \rangle$ versus $i\Delta t$, where $d_j(i)$ is the distance between the jth pair of nearest neighbors (on the reconstructed attractor) after i discrete time steps, the symbol $\langle\cdot\rangle$ denotes an average over all values of j, and Δt is the sampling period of the time series [7].

With short, noisy time series, the aforementioned algorithms can give spurious results; i.e., they can indicate the presence of chaos in systems that are not chaotic. Recently, surrogate data techniques have been developed to detect such "false chaos positives" [9,10]. Surrogate data sets are created by randomizing some property of the original time series. (For example, a surrogate data set can be formed by taking the Fourier transform of a time series, randomizing the phase information, and then taking the inverse Fourier transform; this procedure yields a data set of correlated noise with amplitude spectral characteristics identical to that of the original time series.) The surrogate sets are then processed according to the identical algorithms that are applied to the original time series, and the results are analyzed to test the null hypothesis that the

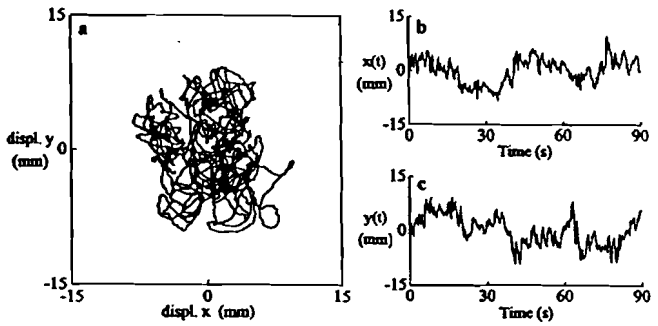

FIG. 1. (a) A typical 90-s center-of-pressure (COP) trajectory, where x and y correspond to the mediolateral and anteroposterior directions, respectively. The corresponding time series are given in (b) and (c). A Kistler 9287 multicomponent force platform and signal conditioner were used to collect COP trajectories on ten healthy subjects—five males and five females—of similar age (19–24 yr, mean 22 ± 2 yr), height (1.60–1.80 m, mean 1.69 ± 0.08 m), and body weight (54.4–77.1 kg, mean 64.3 ± 8.4 kg). Each subject stood barefoot in an upright posture in a standardized stance on the platform for a series of five 90-s trials under eyes-open conditions. The COP signals were antialiased using a second-order low pass filter (with a cutoff frequency of 34.1 Hz) and subsequently sampled at a rate of 100 Hz.

0031-9007/94/73(5)/764(4)$06.00

properties of the surrogate data sets are sufficient to account for the results obtained from the original time series. (The null hypothesis tested with phase-randomized surrogates is that the original time series is correlated noise [9,10].) If the results from the surrogates and the original time series are not significantly different, then the null hypothesis cannot be rejected.

We applied the above techniques to an analysis of the human postural control system. We quantified postural sway in ten subjects (see Fig. 1 caption) by measuring the time-varying displacements of the center of pressure (COP) under each individual's feet (Fig. 1). We tested the null hypothesis that postural sway can be modeled as a correlated noise process. We found that although there appeared to be some structure in the reconstructed COP phase portraits [Fig. 2(a)], similar patterns were apparent in the phase portraits for the phase-randomized surrogates [Fig. 2(b)]. Likewise, the plots of $\ln C(\varepsilon)$ versus $\ln\varepsilon$ for the original COP data [Fig. 2(c)] and the phase-randomized surrogates [Fig. 2(d)] were virtually indistinguishable. In each case, there was no clear linear scaling region of significant length [12] and the slopes of the plots failed to converge with increasing embedding dimension m. (Thus, it was not practical to extract values for D_2.) These qualitative results are those expected for a stochastic system. The Lyapunov exponent results were similar—the plots of $\langle \ln d_j(i) \rangle$ versus $i\Delta t$ for the original posture data [Fig. 2(e)] and the phase-randomized surrogates [Fig. 2(f)] were essentially identical. Although there was no clear linear scaling region in the respective plots, the region between 0.5 and 1.5 s (in particular, for $m < 14$) could be mistaken as appropriate for extracting a positive Lyapunov exponent. We therefore estimated λ_1 over this region for the original COP data and found that the computed values appeared to converge for embedding dimensions of 6, 8, and 10 [Fig. 2(g)]. However, a similar convergence was found in the results for the ensemble of surrogate data sets [Fig. 2(g)]. In addition, this anomalous scaling region, in the original and surrogate data sets, flattened out with increasing embedding dimension [Fig. 2(g)], as would be expected for a stochastic system [7]. For $m > 4$, there were no statistically significant differences between the computed values of λ_1 for the original posture data and the phase-randomized surrogates [Fig. 2(h)]. (The significant differences found for $m \leq 4$ can be attributed in part to the ill-defined nature of the scaling region for these small values of m [Figs. 2(e) and 2(f)].) Similar results were obtained for all 10 subjects (Fig. 3).

Given these findings, we were unable to reject the null hypothesis that postural sway is correlated noise. We therefore concluded that the postural control system should not be modeled as a chaotic process and that it is better represented as a stochastic one. These general results are consistent with those obtained from surrogate analyses of other physiological time series, such as electrocardiograms [9], electroencephalograms [10], and H

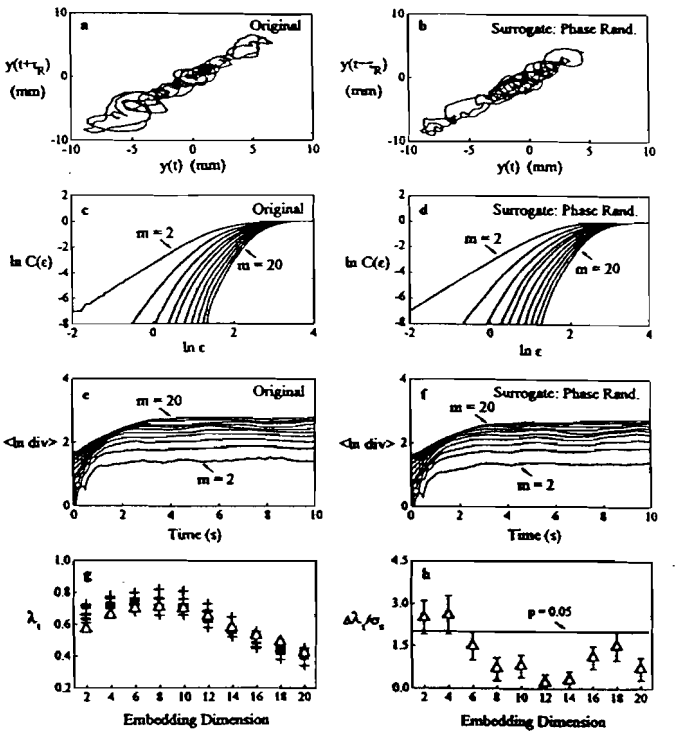

FIG. 2. Dynamical systems analyses of a COP time series and phase-randomized surrogate data sets for a representative subject. All plots, in this figure and other figures, present results for the y-coordinate time series; similar findings were obtained for the x-coordinate time series. (a) A portion of the two-dimensional reconstructed phase portrait for the original COP time series. The reconstruction delay (τ_R) was determined using the reconstruction-expansion approach [11]. (b) As in (a), but for a phase-randomized surrogate data set [9,10] that was generated from the original COP time series in (a). (c) Plots of $\ln C(\varepsilon)$ versus $\ln\varepsilon$ for the original COP time series in (a) (ε is in units of mm). The Grassberger-Procaccia algorithm [5] was used to compute $C(\varepsilon)$, and the reconstruction-expansion approach [11] was used to determine the reconstruction delays for the time-series embeddings. The results for embedding dimensions 2–20, in increments of 2, are shown. (d) As in (c), but for the phase-randomized surrogate data set in (b). (e) Plots of $\langle \ln \text{div} \rangle$ versus time for the COP time series in (a). These plots were generated by computing the average separation of nearest neighbors on the reconstruction attractor [7]. Here "$\langle \ln \text{div} \rangle$" and "Time (s)" are used to denote $\langle \ln d_j(i) \rangle$ and $i\Delta t$, respectively. The results for embedding dimensions 2–20, in increments of 2, are shown. (f) As in (e), but for the phase-randomized surrogate data set in (b). (g) Calculated values of the largest Lyapunov exponent, λ_1, for the original time series (Δ) in (e) and for phase-randomized surrogates (+). An ensemble of ten different phase-randomized surrogate data sets was generated from the original time series and subsequently analyzed. The results are plotted as a function of embedding dimension. All values for λ_1 were extracted from the scaling region between 0.5 and 1.5 s. (h) Significance of the differences between the computed λ_1 values for the original COP time series and the surrogates in (g). The significance values and error bars were calculated according to the techniques described by Theiler *et al.* [10]. Here σ_s is the standard deviation of the λ_1 values for the surrogates and $\Delta\lambda_1$ is the difference between the value of λ_1 for the original COP time series and the mean value of λ_1 for the surrogates. A dashed line is plotted at the significance level which corresponds to a p value of 0.05.

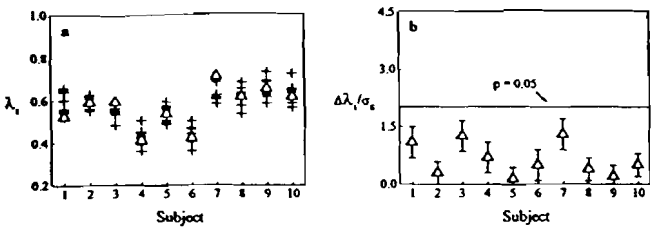

FIG. 3. Calculations of the largest Lyapunov exponent for the experimental population. (a) Calculated values of λ_1 (for an embedding dimension of 12) for representative COP time series (Δ) and phase-randomized surrogates (+) for each of the ten subjects. These values were computed using the techniques described in the legend for Fig. 2(g). In each case, the same scaling region was used to extract λ_1 values from the original COP time series and the surrogates. (b) Significance of the differences between the computed λ_1 values for the original COP time series and the surrogates in (a). This plot was generated using the techniques described in the legend for Fig. 2(h).

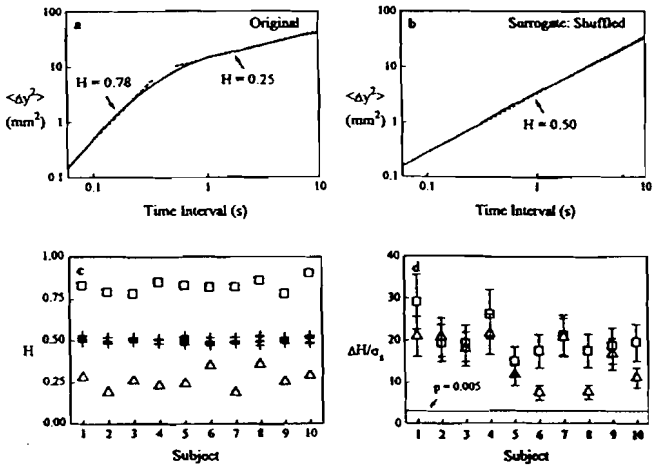

FIG. 4. Random walk analyses of COP time series and shuffled surrogate data sets. (a) A resultant double-logarithmic plot (solid line) of mean square COP displacement ($\langle \Delta y^2 \rangle$) versus time interval ($\tau$) for the representative subject presented in Fig. 2. The displacement analysis was carried out by computing the square of displacements between all pairs of points separated in time by τ. The square displacements were then averaged over the number of τ making up the time series. This process was repeated for increasing values of τ. The results from the 5 trials for each subject were then averaged to obtain a resultant plot of $\langle \Delta y^2 \rangle$ versus τ for each subject. Shown also are the fitted regression lines (dashed lines) for the short-term and long-term scaling regions and the respective computed values for the scaling exponents (H). (b) As in (a), but for shuffled surrogate random-walk data sets that were generated from the original COP time series. (c) Calculated values of H for the short-term (□) and long-term (Δ) scaling regions of the original COP time series and for the shuffled surrogates (+) for each of the ten subjects. For each subject, an ensemble of 10 different shuffled surrogate sets was generated from each of the 5 original COP time series and subsequently analyzed. The regression lines fitted for computation of the respective scaling exponents had r^2 values that ranged from 0.97 to 1.00. (d) Significance of the differences between the computed H values for the original COP time series and the surrogates in (c). These plots were generated using the techniques described in the legend for Fig. 2(h). A dashed line is plotted at the significance level which corresponds to a p value of 0.005.

reflexes [13]. Although deterministic chaos has been observed in perturbed biological preparations, e.g., periodically stimulated chick heart cells [14] and squid axons [15], we are not aware of any documented cases wherein the "steady-state" behavior of a physiological system has been definitively identified (using surrogate data techniques) as an instance of chaos.

Motivated by the above results, we then examined the hypothesis that postural sway can be modeled as a correlated random walk. In a correlated random walk, past increments in displacement are correlated with future increments; i.e., the system has memory. These correlations can be quantified by computing the scaling exponent H from the relation [16]

$$\langle \Delta y^2 \rangle = \langle (y_i - y_{i-\tau})^2 \rangle \sim \tau^{2H},$$

where $\langle \Delta y^2 \rangle$ is mean square displacement and τ is time interval. Scaling exponents can be any real number between 0 and 1. Classical random walks correspond to $H = 0.5$. If $H > 0.5$, then past and future increments are positively correlated, whereas if $H < 0.5$, then past and future increments are negatively correlated [16].

We applied these random walk techniques to the posture data. (Similar correlation techniques have been applied to DNA sequences [17] and heartbeat data [18].) We found that the double-logarithmic plots of mean square COP displacement versus τ exhibited two scaling regions [Fig. 4(a)]: a short-term region over which the time series behaved as a positively correlated random walk ($H > 0.5$) and a long-term region over which it behaved as a negatively correlated random walk ($H < 0.5$) [19]. (A third, distinct region, over which $H \approx 0$, is also expected after a sufficiently large τ given the fact that COP displacements are bounded by the base of support defined by an individual's feet; i.e., for bounded motion, $\langle \Delta y^2 \rangle$ saturates to a constant value after a sufficiently large τ [20]; the time series considered in this study were not long enough to characterize this scaling region reliably.) For the experimental population [Fig. 4(c)], the short-term H values ranged from 0.78 to 0.90 (mean 0.83 ± 0.04), whereas the long-term H values ranged from 0.19 to 0.36 (mean 0.26 ± 0.06). The transition region over which the correlation changed polarity occurred in all subjects at $\tau \approx 1$ s.

In order to determine whether these computed correlations were artefacts of the data-set size and/or the amplitude distribution of the increments, we randomly shuffled the temporal order of the increments [21] making up the COP time series and then recombined the increments to form surrogate random-walk sequences. We found that the double-logarithmic plots of mean square displacement versus τ for the shuffled surrogates displayed only a single scaling region [Fig. 4(b)], as would be expected for an un-

correlated random walk. The H values for the surrogates (range 0.47–0.53, mean 0.50 ± 0.02) were also similar to those expected for a classical random walk [Fig. 4(c)], and they were significantly different from those computed for the original COP time series [Fig. 4(d)]. Thus, we were able to reject the null hypothesis that postural sway is an uncorrelated random walk. These results suggest that the correlations in the COP time series are due to underlying dynamic processes and that they are not artefacts of the analysis. We therefore concluded that postural sway can be modeled as a system of bounded, correlated random walks.

From a physiological standpoint, the presence of short-range positive correlations in the COP data suggests that the postural control system utilizes open-loop control mechanisms over short-term intervals of time ($\tau < 1$ s) and small displacements. That is, the system allows the COP to "drift" for some time and/or displacement. This novel finding, which suggests that the system allows a certain amount of "sloppiness" in balance control, challenges the generally accepted notion that erect stance is always regulated by the action of feedback mechanisms [22]. It is important to note, however, that our analyses do not exclude the role of feedback mechanisms, such as the visual, vestibular, and proprioceptive systems, in the regulation of upright stance. In fact, the presence of longer-range negative correlations in the COP data suggests that closed-loop control mechanisms are utilized over long-term intervals of time ($\tau > 1$ s) and large displacements. That is, after some time and/or displacement, the postural control system shifts the COP back towards a relative equilibrium position. The integration of open-loop control schemes with closed-loop feedback mechanisms for balance regulation may have evolved to account for feedback-loop delays and inherent noise in the system (e.g., due to inherent muscle force fluctuations [23]), and to simplify the task of integrating vast amounts of sensory information when the body is not in jeopardy of instability.

We thank Ann Pavlik and Mike Rosenstein for their assistance with software development and figure preparation. This work was supported by the National Science Foundation and the Rehab R&D Service of the Department of Veterans Affairs.

*Author to whom correspondence should be addressed. Phone: (617) 353-9757. FAX: (617) 353-5737. Electronic address: collins@buenga.bu.edu

[1] L. Glass and M.C. Mackey, *From Clocks to Chaos* (Princeton Univ. Press, Princeton, 1988).
[2] P.E. Rapp *et al.*, Phys. Lett. A **110**, 335 (1985); A. Babloyantz, J.M. Salazar, and C. Nicolis, Phys. Lett. A **111**, 152 (1985); A. Babloyantz and A. Destexhe, Proc. Natl. Acad. Sci. **83**, 3513 (1986); G.W. Frank *et al.*, Physica (Amsterdam) **46D**, 427 (1990); J. Fell, J. Röschke, and P. Beckmann, Biol. Cybern. **69**, 139 (1993).
[3] C. Gantert, J. Honerkamp, and J. Timmer, Biol. Cybern. **66**, 479 (1992).
[4] J.J. Collins and C.J. De Luca, Exp. Brain Res. **95**, 308 (1993).
[5] P. Grassberger and I. Procaccia, Phys. Rev. Lett. **50**, 346 (1983).
[6] A. Wolf *et al.*, Physica (Amsterdam) **16D**, 285 (1985).
[7] M.T. Rosenstein, J.J. Collins, and C.J. De Luca, Physica (Amsterdam) **65D**, 117 (1993).
[8] N.H. Packard *et al.*, Phys. Rev. Lett. **45**, 712 (1980); F. Takens, in *Dynamical Systems and Turbulence*, edited by D. Rand and L.-S. Young (Springer-Verlag, Berlin, 1981), pp. 366–381.
[9] D.T. Kaplan and R.J. Cohen, Circulation Res. **67**, 886 (1990).
[10] J. Theiler *et al.*, Physica (Amsterdam) **58D**, 77 (1992).
[11] M.T. Rosenstein, J.J. Collins, and C.J. De Luca, Physica (Amsterdam) **73D**, 82 (1994).
[12] P.E. Rapp *et al.*, Phys. Rev. E **47**, 2289 (1993).
[13] S.J. Schiff and T. Chang, Biol. Cybern. **67**, 387 (1992).
[14] M.R. Guevara, L. Glass, and A. Shrier, Science **214**, 1350 (1981).
[15] G. Matsumoto *et al.*, Phys. Lett. A **123**, 162 (1987).
[16] J. Feder, *Fractals* (Plenum, New York, 1988).
[17] C.-K. Peng *et al.*, Nature (London) **356**, 168 (1992).
[18] C.-K. Peng *et al.*, Phys. Rev. Lett. **70**, 1343 (1993).
[19] The maximum time interval considered in the random walk analysis was 10 s. This value was chosen because it was sufficient to characterize the long-term scaling region of the postural control system (as determined from a pilot study involving larger data sets, e.g., 240-s COP time series) and the inclusion of longer time intervals in the present analyses may have introduced spurious or unreliable results, given that we only considered 90-s COP time series.
[20] J. Theiler, Phys. Lett. A **155**, 480 (1991).
[21] J.A. Scheinkman and B. LeBaron, J. Business **62**, 311 (1989).
[22] A. Ishida and S. Miyazaki, IEEE Trans. Biomed. Eng. **34**, 1 (1987).
[23] C.J. De Luca *et al.*, J. Physiol. **329**, 129 (1982).